Molecular Biology of the Cell
Vol. 18, 3993–4002, October 2007

Prophase Microtubule Arrays Undergo Flux-like Behavior in Mammalian Cells[D] [V]

Nick P. Ferenz and Patricia Wadsworth

Department of Biology and Program in Molecular and Cellular Biology, University of Massachusetts, Amherst, MA 01003

Submitted May 8, 2007; Revised July 12, 2007; Accepted July 20, 2007
Monitoring Editor: Kerry Bloom

In higher eukaryotic cells, microtubules within metaphase and anaphase spindles undergo poleward flux, the slow, poleward movement of tubulin subunits through the spindle microtubule lattice. Although a number of studies have documented this phenomenon across a wide range of model systems, the possibility of poleward flux before nuclear envelope breakdown (NEB) has not been examined. Using a mammalian cell line expressing photoactivatable green fluorescent protein (GFP)-tubulin, we observe microtubule motion, both toward and away from centrosomes, at a wide range of rates (0.5–4.5 μm/min) in prophase cells. Rapid microtubule motion in both directions is dynein dependent. In contrast, slow microtubule motion, which occurs at rates consistent with metaphase flux, is insensitive to inhibition of dynein but sensitive to perturbation of Eg5 and Kif2a, two proteins with previously documented roles in flux. Our results demonstrate that microtubules in prophase cells are unexpectedly dynamic and that a subpopulation of these microtubules shows motion that is consistent with flux. We propose that the marked reduction in rate and directionality of microtubule motion from prophase to metaphase results from changes in microtubule organization during spindle formation.

INTRODUCTION

After spindle formation, microtubule marking experiments have revealed a unique form of motion called flux, which results from the coordinated addition and loss of tubulin subunits at opposite ends of spindle microtubules during metaphase (Mitchison, 1989). During anaphase, flux contributes to chromosome-to-pole motion, although the extent of flux-dependent chromosome motion varies by model system (Rogers *et al*., 2005). To date, flux has been observed in all eukaryotic cells examined except yeast (Mitchison, 1989; Sawin and Mitchison, 1991; Mitchison and Salmon, 1992; Maddox *et al*., 2000, 2002; LaFountain *et al*., 2004); and recently, a number of contributing molecular components have been identified, namely, Eg5 and Kif2a.

Eg5 is a homotetrameric, plus end-directed member of the kinesin-5 family that is capable of sliding antiparallel microtubules relative to one another in vitro (Kapitein *et al*., 2005). Kif2a is a microtubule destabilizing member of the kinesin-13 family that lacks inherent motility (Desai *et al*., 1999). Both proteins are enriched at spindle poles during metaphase, although Eg5 additionally stains spindle microtubules (Kapoor *et al*., 2000; Ganem and Compton, 2004). Importantly, each of these proteins has been implicated in the flux mechanism. Inhibition of Eg5, for example, has been shown to reduce the rate of flux in mammalian cells (Cameron *et al*., 2006) and to eliminate flux in *Xenopus* egg extracts (Miyamoto *et al*., 2004; Shirasu-Hiza *et al*., 2004). Likewise, the perturbation of Kif2a has been reported to abolish flux in mammalian cells (Ganem *et al*., 2005), *Drosophila* embryos (Rogers *et al*., 2004) and *Xenopus* egg extracts (Gaetz and Kapoor, 2004). Mechanistically, flux has been modeled as a combination of Kif2a-mediated depolymerization of microtubule minus ends and Eg5-mediated sliding of overlapping, antiparallel microtubules. Recently, this model has been challenged by new data documenting the continuation of flux, albeit at reduced rates, in mammalian monopolar spindles lacking antiparallel microtubules (Cameron *et al*., 2006). Considering these data, as well as the centrosomal enrichment of Eg5, it is possible that in mammalian cells, Eg5 may contribute to flux by reeling in and feeding microtubules to the Kif2a depolymerase as suggested previously (Cassimeris, 2004; Gadde and Heald, 2004).

Despite the extensive work concerning the occurrence and mechanics of flux, all studies have been conducted after nuclear envelope breakdown (NEB), leaving the possibility of prophase flux unaddressed. Here, we examine microtubule behavior after photoactivation of green fluorescent protein (GFP)-tubulin in prophase cells, and we compare the results with experiments performed in early prometaphase and metaphase cells. We show that prophase microtubules are remarkably dynamic, because photoactivated marks move toward and away from spindle poles at a wide range of rates, and that the variability of this motion decreases as mitosis progresses, with only slow, poleward-directed motion remaining at metaphase. Additionally, a subset of prophase and early prometaphase microtubule motion occurs at rates consistent with flux, and it is sensitive to perturbation of Eg5 and Kif2a, but not dynein. These data demonstrate that a population of microtubules in prophase and early prometaphase cells exhibits behavior consistent with flux.

This article was published online ahead of print in *MBC in Press* (http://www.molbiolcell.org/cgi/doi/10.1091/mbc.E07–05–0420) on August 1, 2007.

[D] [V] The online version of this article contains supplemental material at *MBC Online* (http://www.molbiolcell.org).

Address correspondence to: Patricia Wadsworth (patw@bio.umass.edu).

Abbreviations used: AP, away from a spindle pole; NEB, nuclear envelope breakdown; P, toward a spindle pole.

MATERIALS AND METHODS

Materials

All materials for cell culture were obtained from Sigma-Aldrich (St. Louis, MO) with the exception of Opti-MEM, which was obtained from Invitrogen (Carlsbad, CA) and fetal bovine serum, which was obtained from Atlanta Biologicals (Norcross, GA). Unless otherwise noted, all other chemicals were obtained from Sigma-Aldrich (St. Louis, MO).

Cell Culture

LLC-Pk1 cells expressing photoactivatable (PA)-GFP-tubulin were cultured as described previously (Tulu *et al*., 2003). Cells were plated on glass coverslips (Corning Life Sciences, Acton, MA) 2 d before imaging. For live imaging, cells were mounted in chambers containing non-CO_2 minimal essential medium supplemented with 0.3 U/ml Oxyrase (EC Oxyrase, Oxyrase, Mansfield, OH), and they were maintained at ~37°C.

Inhibitors

p150-CC1 plasmid, a gift from Dr. T. Kapoor (The Rockefeller University, New York, NY), was prepared according to protocol (King *et al*., 2003). After dilution with injection buffer (50 nM K-Glu and 1 mM $MgCl_2$, pH 7.0), it was injected at 15 μM. Monastrol was used at 200 μM. Kif2a and MCAK antibodies, kind gifts from Drs. D. Compton (Dartmouth Medical School, Hanover, NH) and C. Walczak (Indiana University, Bloomington, IN), respectively, were combined 1:1 at full strength and injected.

Immunofluorescence

Cells were rinsed twice in calcium and magnesium-free phosphate-buffered saline (PBS), fixed in either paraglutaraldehyde (4.0% paraformaldehyde, 0.10% glutaraldehyde, and 0.5% Triton X-100 in calcium- and magnesium-free PBS) for 5 min or glutaraldehyde (0.25% glutaraldehyde in calcium- and magnesium-free PBS) for 1 min, treated with 1 mg/ml sodium borohydride for 10 min, and rehydrated in calcium- and magnesium-free PBS containing 0.1% Tween and 0.02% sodium azide. For the glutaraldehyde fixation, cells were additionally lysed in Karsenti's [0.5% Triton X-100, 80 mM piperazine-*N*,*N*′-bis(2-ethanesulfonic acid), 1 mM $MgSO_4$, and 5 mM EGTA] for 1 min after the initial glutaraldehyde incubation, and then they were fixed again for 5–10 min before sodium borohydride treatment. The following primary antibodies were used in these experiments: YL½ (Accurate Chemical, Westbury, NY) used at 1:2; anti-Eg5, gift from Dr. D. Compton (Dartmouth Medical School, Hanover, NH) used at 1:200; and anti-Kif2a (Novus Biologicals, Littleton, CO) used at 1:10,000. Incubations with primary antibodies were performed overnight at room temperature or for 1 h at 37°C. Cy3- (Jackson ImmunoResearch Laboratories, West Grove, PA) or fluorescein isothiocyanate-labeled (Sigma-Aldrich, St. Louis, MO) secondary antibodies were used at the recommended dilution for 30 or 90 min at room temperature, respectively. Coverslips were mounted in Vectashield (Vector Laboratories, Burlingame, CA) and sealed with nail polish.

Image Acquisition

Images were acquired using a Nikon Eclipse TE 300 microscope equipped with a 100× phase, numerical aperture 1.4 objective lens, a spinning disk confocal scan head (PerkinElmer-Cetus, Wellesley, MA), and a Hamamatsu Orca ER cooled charge-coupled device camera (Hamamatsu, Bridgewater, NJ). All images were taken with a single wavelength (488) filter cube. Image acquisition was controlled by MetaMorph software (Molecular Devices, Sunnyvale, CA). Time-lapse sequences were acquired at 5-s intervals using an exposure time of 800 ms. Z-stacks were acquired at 0.2-μm steps using an exposure time of 800 ms.

For photoactivation experiments, cells were photoactivated (under the nucleus during prophase and along spindle fibers post-NEB) by a 5-s exposure to 413-nm light using an X-Cite 120 light source (EXFO America, Plano, TX) and a D405/20 filter cube (Chroma Technology, Rockingham, VT). The area of photoactivation was restricted using a slit (Lennox Laser, Glen Arm, MD) mounted in a Ludl filter wheel placed in a conjugate image plane in the epi-illumination light path. To activate the entire field of view, an open position in the filter wheel was selected. After photoactivation, confocal image acquisition proceeded as described above. Images were acquired ~1–10 min after p150-CC1 injection, ~5–15 min after Kif2a/MCAK injection, and ~1–3.5 h after monastrol treatment.

Images of fixed cells were acquired by capturing optical sections every 0.2 μm using exposure times of 200–400 ms (at 488 nm) and 800 ms (at 568 nm), and they were displayed as maximum intensity projections. Deconvolved images were acquired using AutoDeblur & AutoVisualize software, version 9.3.6 (AutoQuant Imaging, Watervliet, NY).

Data Analysis

Immediately after each time-lapse sequence, the entire cell was photoactivated, and a Z-stack was acquired to determine the location of each centrosome. Frequently, centrosomes (or spindle poles, depending on the mitotic stage) in early mitotic cells were located in different focal planes. However, because the relative location of the initial photoactivated region could be compared in X, Y, and Z to the fully photoactivated Z-stack, photoactivated marks could be determined to be associated with microtubules of a particular centrosome. With a single centrosome as a reference point, motion could be categorized as toward that particular centrosome, not away from the other (and vice versa). To calculate rates of motion, a rectangular box, typically 11 pixels in height (defined as the dimension perpendicular to the long axis of the photoactivated mark), was placed around a fluorescent mark of interest. The dimensions of the box were selected so that, during the time lapse, the mark of interest remained within the defined region. Montages were created for each boxed region, and rates were extrapolated from the montage's slope. All data were plotted using Excel (Microsoft, Redmond, WA). All statistics were analyzed using a Student's *t* test.

RESULTS

Metaphase Flux in LLC-Pk1-PA Cells

To determine whether microtubules undergo flux during prophase, flux was first characterized in metaphase LLC-Pk1 cells. To do this, a permanent cell line expressing photoactivatable GFP-tubulin (hereafter LLC-Pk1-PA) was used (Patterson and Lippincott-Schwartz, 2002; Tulu *et al*., 2003). Metaphase cells were photoactivated, and time-lapse sequences of the resulting fluorescent marks were acquired (Figure 1A and Supplemental Video 1). The location of each centrosome was identified from a Z-stack obtained after the entire cell was photoactivated, and each clear mark was assigned a rate and directionality, scored as either toward (P) or away from (AP) the spindle poles (see *Materials and Methods*).

In metaphase cells, photoactivated marks on spindle microtubules moved poleward between 0.50 and 2.24 μm/min, with an average rate of 1.37 μm/min (Figure 1B and Table 1). AP motion was not detected. Although published rates of flux in LLC-Pk1 cells are significantly lower than the rate reported here (Mitchison, 1989; Zhai *et al*., 1995), those measurements were based on data collected at 30°C. Indeed, when photoactivations were performed at this reduced temperature, the average rate of metaphase flux decreased to 0.75 μm/min, a value more in line with the literature. Furthermore, despite the substantial difference between the rates of chromosomal oscillations in the spindle center (1.96 μm/min) and periphery (1.45 μm/min), flux rates were identical regardless of location (unpublished data), consistent with recent observations in PtK1 cells (Cameron *et al*., 2006).

Prophase Microtubule Motion Is Extremely Variable

Next, photoactivations were performed before NEB to examine microtubule behavior during early mitosis (Figure 1A and Supplemental Video 2). In most prophase cells, the data revealed a surprisingly wide distribution of rates (0.50–4.49 μm/min) and the co-occupancy of nearly each populated range with both directionalities of motion (Figure 1B). Approximately 61% of this motion was P, and ~39% was AP (Table 2). This distribution did not seem to depend on the location of the photoactivation, because activations gave similar results regardless of the distance from the centrosomes. However, in very early prophase cells with little chromatin condensation, photoactivated marks were static, indicating that the onset of microtubule motion is abrupt and takes place between mid- and late prophase (unpublished data).

To establish a link between our prophase data and the earliest mitotic stage at which flux is known to occur (late prometaphase cells with nearly all chromosomes aligned at the metaphase plate), photoactivations also were performed during early prometaphase (i.e., post-NEB cells with numerous unaligned chromosomes) (Figure 1A and Supplemental Video 3). In such cells, the distribution of rates was similar to that seen during prophase (0.50–3.49 μm/min), although

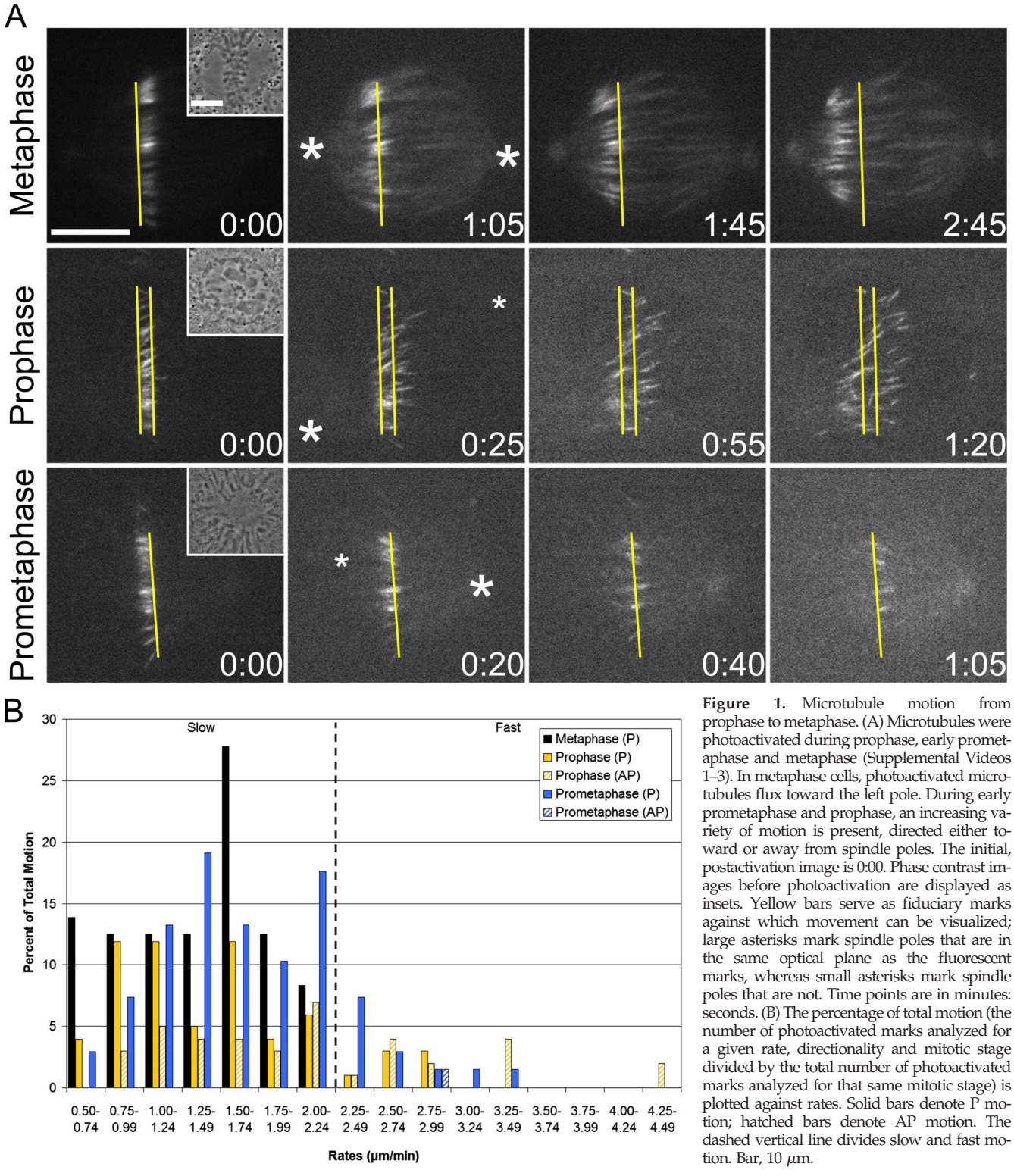

Figure 1. Microtubule motion from prophase to metaphase. (A) Microtubules were photoactivated during prophase, early prometaphase and metaphase (Supplemental Videos 1–3). In metaphase cells, photoactivated microtubules flux toward the left pole. During early prometaphase and prophase, an increasing variety of motion is present, directed either toward or away from spindle poles. The initial, postactivation image is 0:00. Phase contrast images before photoactivation are displayed as insets. Yellow bars serve as fiduciary marks against which movement can be visualized; large asterisks mark spindle poles that are in the same optical plane as the fluorescent marks, whereas small asterisks mark spindle poles that are not. Time points are in minutes: seconds. (B) The percentage of total motion (the number of photoactivated marks analyzed for a given rate, directionality and mitotic stage divided by the total number of photoactivated marks analyzed for that same mitotic stage) is plotted against rates. Solid bars denote P motion; hatched bars denote AP motion. The dashed vertical line divides slow and fast motion. Bar, 10 μm.

AP motion was practically undetectable (Figure 1B). Approximately 99% of all early prometaphase motion was P, and ~1% was AP (Table 2).

In each of the above-mentioned cases, a subpopulation of photoactivated marks could be seen moving poleward at rates consistent with metaphase flux (0.50–2.24 μm/min). To directly analyze this subset, motion was classified not only as P or AP but also as slow (rates within the metaphase flux range) or fast (rates beyond the metaphase flux range). Using these criteria, the average rates of slow P (flux-like) motion in prophase and early prometaphase cells were not significantly different from the metaphase flux value (Table 1). We therefore hypothesized that early mitotic slow P motion represented flux.

Table 1. Average rates (μm/min) of photoactivated marks in mitotic LLC-Pk1-PA cells

	Slow P	Fast P	Slow AP	Fast AP
Control				
Prophase	1.34 ± 0.45	**2.69 ± 0.24**	**1.56 ± 0.46**	**3.12 ± 0.65**
Prometaphase	1.52 ± 0.45	2.63 ± 0.36		≤2 rates
Metaphase	**1.37 ± 0.47**			
p150-CC1				
Prophase	1.24 ± 0.46	≤2 rates	1.35 ± 0.51	≤2 rates
Prometaphase	1.32 ± 0.46		≤2 rates	≤2 rates
Metaphase	1.22 ± 0.36			
Kif2a/MCAK				
Prophase	1.02 ± 0.28[a]	2.68 ± 0.58	1.23 ± 0.59	≤2 rates
Prometaphase	1.01 ± 0.30[a]			
Metaphase	1.17 ± 0.29[b]			
Monastrol				
Prophase	1.41 ± 0.33	≤2 rates	1.55 ± 0.43	3.43 ± 0.55
Monopole	1.06 ± 0.42[c]			
Metaphase	0.95 ± 0.18[a]			

Rates ± SDs. Unless otherwise indicated, values in any one column are not statistically different from that column's control value (denoted in bold).

[a] Statistically significant at $p = 0.001$.

[b] Statistically significant at $p = 0.05$.

[c] Statistically significant at $p = 0.01$.

Flux-like Motion Is Dynein Independent

Small molecule inhibition and RNA interference knockdown experiments have established flux as a dynein-independent event (Sawin and Mitchison, 1991; Maiato *et al*., 2005). In contrast, rapid inward motion (i.e., sliding) of peripheral microtubules has been shown to depend on dynein (Rusan *et al*., 2002). We predicted that if the slow P component of early mitotic motion corresponded to flux, it too would be dynein-independent. To test this, LLC-Pk1-PA cells were microinjected before photoactivation with p150-CC1, a protein fragment that binds dynein IC and disrupts dynein/dynactin interactions (Quintyne *et al*., 1999; Gaetz and Kapoor, 2004) (Figure 2A and Supplemental Videos 4 and 5). Importantly, we found that, as in Ptk1 cells, p150-CC1 does not mislocalize Kif2a in LLC-Pk1 cells (unpublished data) as it does in *Xenopus* egg extracts (Gaetz and Kapoor, 2004; Cameron *et al*., 2006). Moreover, p150-CC1 does not disrupt centrosome integrity during the experimental time course.

As predicted, slow P motion in prophase, early prometaphase, and metaphase cells was unaffected by dynein inhibition. Average rates were not significantly different from the control value (Table 1), and there was no noticeable change in the frequency of this motion (Table 2). In contrast, microinjection of p150-CC1 essentially abolished all fast motion, both toward and away from the poles, during prophase and early prometaphase (Figure 2B). In control prophase cells, ~20% of all motion was fast, and this was decreased to ~5% after injection (Table 2). In control early prometaphase cells, ~16% of all motion was fast, and this was decreased to ~3% after injection (Table 2). The residual fast motion may result from incomplete inhibition of dynein, or it may be the consequence of other motors that generate rapid movement (DeLuca *et al*., 2001). Consistent with previous reports (Salina *et al*., 2002), NEB was delayed in injected cells (unpublished data). These data demonstrate that fast P and AP motion is dynein dependent, and they support a model in which microtubules can be the cargo of cytoplasmic dynein (Rusan *et al*., 2002; Wadsworth and Khodjakov, 2004). Additionally, the insensitivity of slow P motion to dynein inhibition is consistent with flux; however, it does not exclude dynein-independent sliding as the underlying basis for such motion.

Kinesin-13 Inhibition Decreases the Rate of Flux-like Motion

Experiments in mammalian tissue culture cells, *Drosophila* embryos, and *Xenopus* egg extracts have demonstrated that members of the kinesin-13 family contribute to poleward flux (Gaetz and Kapoor, 2004; Rogers *et al*., 2004; Ganem *et al*., 2005). Accordingly, we predicted that the rate of slow P motion would be sensitive to inhibition of Kif2a, a mammalian kinesin-13. To test this, the strategy of Ganem *et al*. (2005) was followed by microinjecting a mixture of Kif2a and MCAK antibodies before photoactivation (Figure 3A and Supplemental Videos 6 and 7). Such injections resulted in extensive astral microtubule formation and kinetochore fiber buckling, demonstrating that the antibodies alter microtubule dynamics in LLC-Pk1-PA cells (Figure 3B).

As anticipated, the average rates of prophase, early prometaphase, and metaphase slow P motion were significantly reduced from the control value (Table 1). However, the overall distribution of rates remained unaltered in prophase cells, and it was only slightly modified in early prometaphase cells (Figure 3C and Table 2). These data demonstrate that prophase and early prometaphase slow P motion is affected in an identical manner as metaphase flux. Double label immunofluorescence further shows that Kif2a localizes to centrosomes during prophase and spindle poles after NEB in LLC-Pk1-PA cells and that numerous microtubules terminate at the centrosome (Supplemental Figure S1). These observations, in addition to the well-established minus end depolymerizing activity of Kif2a, suggest that slow poleward motion in prophase cells corresponds to flux.

Eg5 Inhibition Decreases the Frequency of Flux-like Motion during Prophase

Evidence from *Xenopus* and mammalian systems has indicated the involvement of Eg5 in flux (Miyamoto *et al*., 2004;

Table 2. Distribution of prophase and early prometaphase microtubule motion for each experimental condition

	Prophase			Prometaphase		
	Slow	Fast	Totals	Slow	Fast	Totals
Control						
P (%)	54	7	61	84	15	99
	n = 55	n = 7	n = 62	n = 57	n = 10	n = 67
AP (%)	26	13	39	0	1	1
	n = 26	n = 13	n = 39	n = 0	n = 1	n = 1
Totals (%)	80	20	20 cells	84	16	20 cells
	n = 81	n = 20		n = 57	n = 11	
p150-CC1[a]						
P (%)	55	1	56	91	0	91
	n = 30 (50)	n = 1 (2)	n = 31 (52)	n = 30 (67)	n = 0 (0)	n = 30 (67)
AP (%)	40	4	44	6	3	9
	n = 22 (37)	n = 2 (3)	n = 24 (40)	n = 2 (4)	n = 1 (2)	n = 3 (6)
Totals (%)	95	5	12 cells	97	3	9 cells
	n = 52 (87)	n = 3 (5)		n = 32 (71)	n = 1 (2)	
Kif2a/MCAK[b]						
P (%)	50	13	63	100	0	100
	n = 15 (38)	n = 4 (10)	n = 19 (48)	n = 27 (60)	n = 0 (0)	n = 27 (60)
AP (%)	33	4	37	0	0	0
	n = 10 (25)	n = 1 (3)	n = 11 (28)	n = 0 (0)	n = 0 (0)	n = 0 (0)
Totals (%)	83	17	8 cells	100	0	9 cells
	n = 25 (63)	n = 5 (13)		n = 27 (60)	n = 0 (0)	
Monastrol[c]						
P (%)	12	2	14	100	0	100
	n = 5 (10)	n = 1 (2)	n = 6 (12)	n = 31 (56)	n = 0 (0)	n = 31 (56)
AP (%)	55	31	86	0	0	0
	n = 23 (46)	n = 13 (26)	n = 36 (72)	n = 0 (0)	n = 0 (0)	n = 0 (0)
Totals (%)	67	33	10 cells	100	0	11 cells
	n = 28 (56)	n = 14 (28)		n = 31 (56)	n = 0 (0)	

To make the number of measured marks comparable between treatments involving a variable number of analyzed cells, the observable n for each experimental treatment has been supplemented with a value in parentheses that represents the number of marks expected in 20 cells (the number of cells analyzed for both prophase and early prometaphase controls).

[a] p150-CC1 does not alter the frequency of slow P motion. During prophase, 50 slow P marks would be expected in 20 injected cells (similar to the 55 slow P marks recorded in controls). During early prometaphase, 67 slow P marks would be expected in 20 injected cells (similar to the 57 slow P marks recorded in controls).

[b] Kif2a/MCAK injection does not alter the prophase distribution of rates but slightly alters the early prometaphase distribution. In control prophase cells, ~60% of all motion is P (~40% is AP) and ~80% is slow (~20% is fast). This is identical to the distribution after injection. In control early prometaphase cells, ~100% of all motion is P and ~85% is slow (~15% is fast). After injection, 100% of all motion is slow P.

[c] Monastrol treatment causes a true decrease in prophase P motion, evidenced by the 12 marks expected to move poleward in 20 monastrol-treated cells (compared with the 62 marks recorded in controls), and a true increase in AP motion, evidenced by the 72 marks expected to move away from the pole in 20 monastrol-treated cells (compared with the 39 marks recorded in controls).

Shirasu-Hiza *et al*., 2004; Cameron *et al*., 2006). For this reason, we predicted that the rate of slow P motion would be reduced after inhibition of Eg5. To test this, Eg5 activity was inhibited using the small molecule monastrol (Mayer *et al*., 1999), and cells were photoactivated in the continued presence of the inhibitor (Figure 4A and Supplemental Video 8). Prophase cells were imaged through NEB to ensure the formation of monopolar spindles, the hallmark of Eg5 inhibition (Figure 4B).

Unexpectedly, the rate of slow P motion during prophase was not different from the control value (Table 1); however, the frequency of this particular motion was strongly decreased from ~54% in controls to ~12% (Table 2). In fact, across the full range of rates (which was indistinguishable from the untreated prophase range), the proportion of P and AP motion was significantly shifted (Figure 4C). Approximately 14% of all motion was P (compared with ~61% in controls), and ~86% was AP (compared with ~39% in controls) (Table 2). Importantly, both the decrease in P motion and the increase in AP motion represent true shifts; neither are artificial consequences of changes in the opposing directionality (Table 2). These data reveal that, during prophase, Eg5 activity is required to generate slow P motion and maintain a balance between P and AP motion. Because Eg5 is highly concentrated at centrosomes during prophase (Supplemental Figure S1A), these results favor a model where Eg5 functions at least in part to reel in microtubules at spindle poles (Cassimeris, 2004; Gadde and Heald, 2004), thus accounting for the decreased frequency of flux-like motion.

Eg5 Inhibition Decreases the Rate of Flux-like Motion after NEB

Last, we examined microtubule behavior in monastrol-treated LLC-Pk1-PA cells that had undergone NEB and formed monopolar spindles (Figure 4A and Supplemental Video 9). In 11 of 14 monopoles examined, we found that photoactivated marks moved exclusively in the P direction, confirming that flux occurs in monopolar spindles (Cameron *et al*., 2006), across a range of rates slightly reduced from controls (Figure 4C). In the remaining three cells, no motion

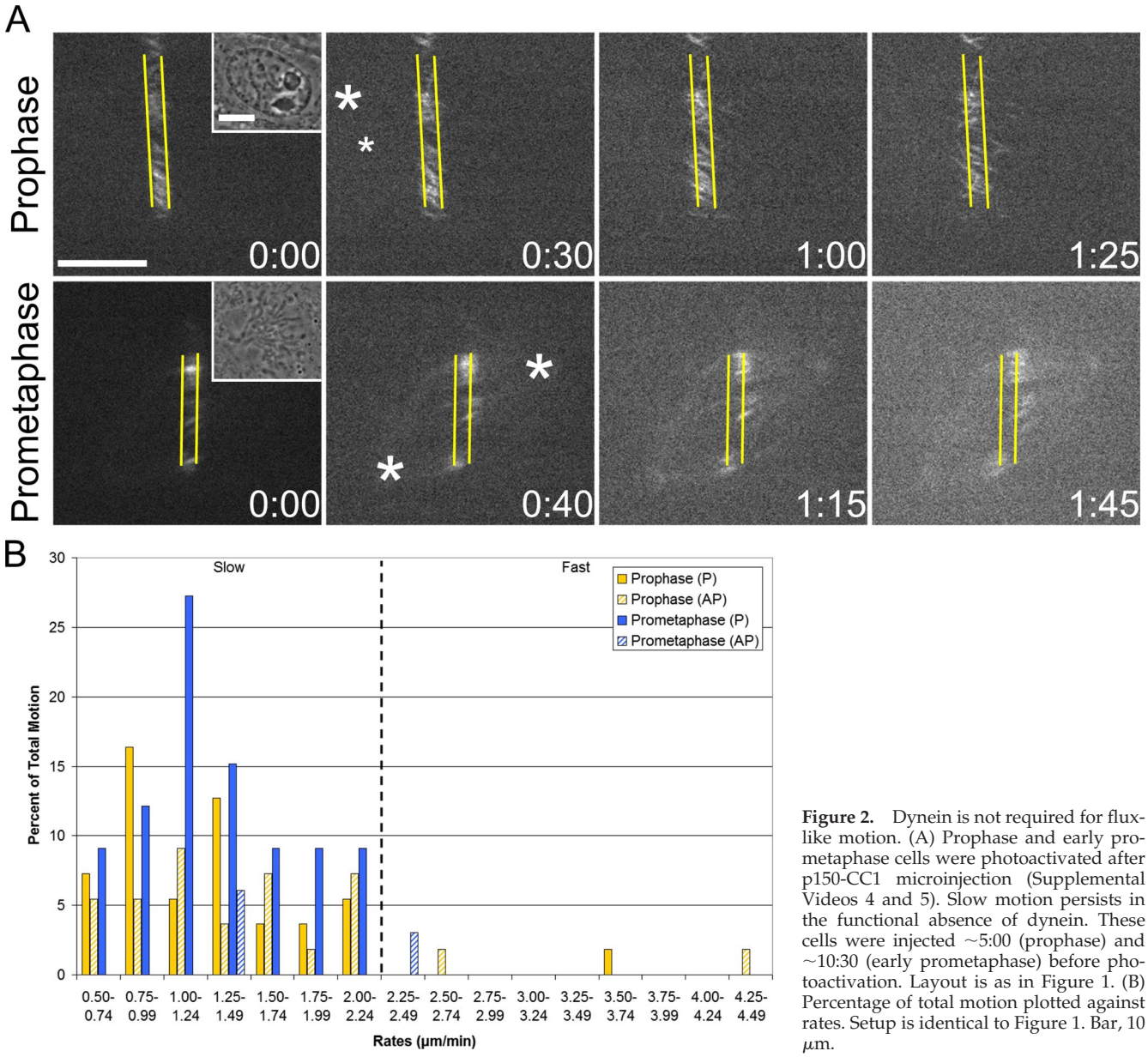

Figure 2. Dynein is not required for flux-like motion. (A) Prophase and early prometaphase cells were photoactivated after p150-CC1 microinjection (Supplemental Videos 4 and 5). Slow motion persists in the functional absence of dynein. These cells were injected ~5:00 (prophase) and ~10:30 (early prometaphase) before photoactivation. Layout is as in Figure 1. (B) Percentage of total motion plotted against rates. Setup is identical to Figure 1. Bar, 10 μm.

was detected. Unlike prophase cells, the average rate of slow P motion in monopoles was significantly reduced compared with the control value (Table 1). Likewise, the rate of slow P motion in monastrol-treated bipolar spindles that resisted collapse was also significantly reduced (Table 1). These data agree with previous reports examining the response of flux to monastrol treatment (Cameron *et al.*, 2006) and again favor a feeder-chipper model (Cassimeris, 2004; Gadde and Heald, 2004) as Eg5 concentrates at spindle poles during both early prometaphase and metaphase (Supplemental Figure S1A). The presence of additional factors aiding Eg5 in the task of delivering microtubules to the depolymerase may explain why post-NEB cells do not display a decrease in the frequency of flux-like motion.

DISCUSSION

The results of our experiments demonstrate that microtubules in prophase cells are remarkably dynamic, undergoing motion toward and away from centrosomes at variable rates, and that a subset of this motion is comparable with metaphase flux. These data raise two important and related questions: does slow P motion in prophase cells correspond to flux, and what accounts for the variation in rate and directionality of prophase microtubule motion?

Does Slow P Motion Correspond to Flux?

The observation that slow P motion during prophase and early prometaphase shows identical sensitivity to antibody-mediated inhibition of kinesin-13 proteins as slow P motion (i.e., flux) during metaphase provides strong evidence that these motions are driven by the same, or a very similar, molecular mechanism. Alternative explanations for slow P motion, such as microtubule–microtubule or microtubule–spindle matrix sliding via molecular motors, are inconsistent with the kinesin-13 inhibition data, as such mechanisms would not be sensitive to inhibition of a depolymerase. Additionally, the behavior of motile marks in prophase cells

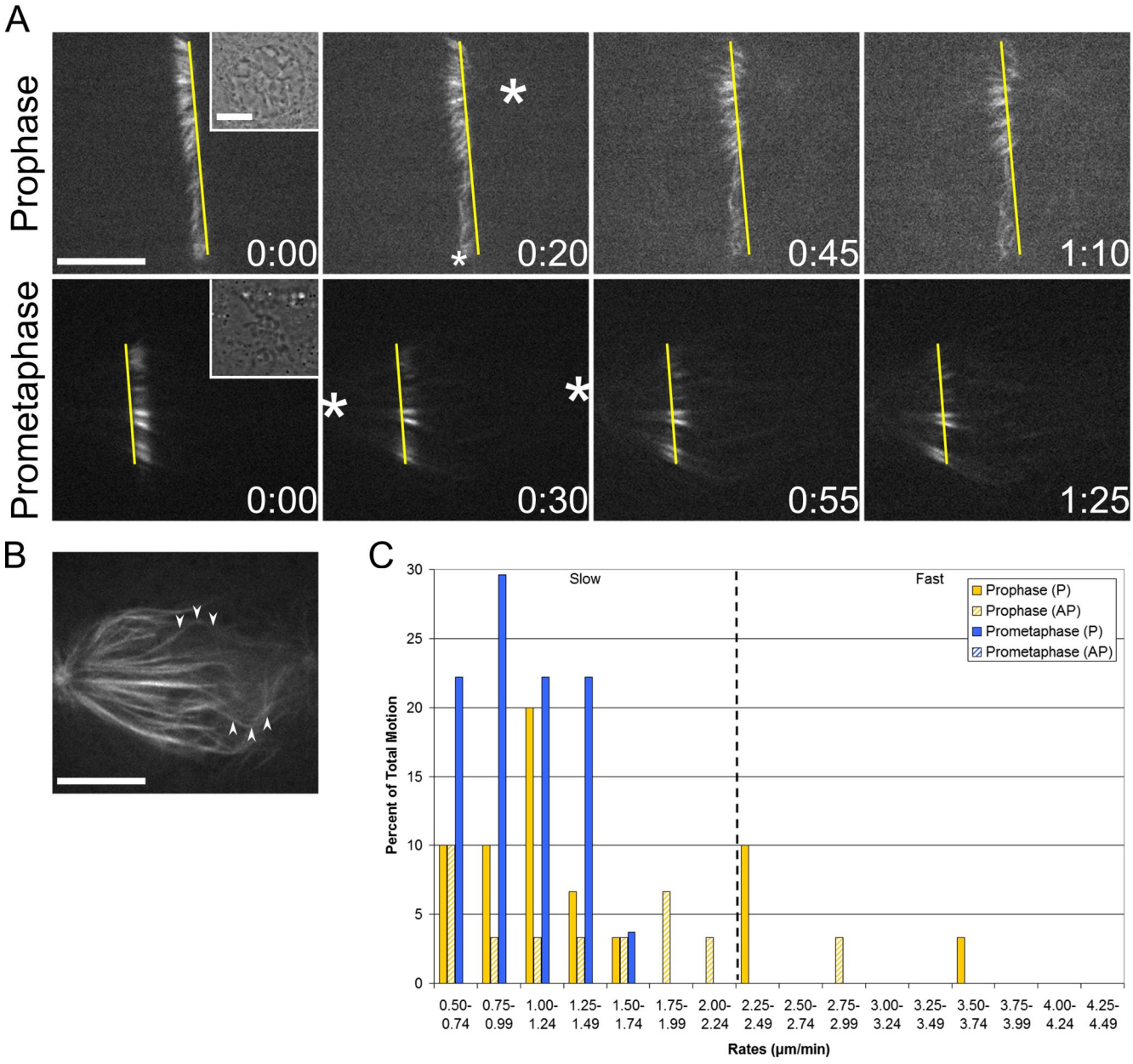

Figure 3. The rate of flux-like motion is sensitive to kinesin-13 inhibition. (A) Prophase and early prometaphase cells were photoactivated after Kif2a/MCAK microinjection (Supplemental Videos 6 and 7). Slow P motion continues, but at a reduced rate. These cells were injected ~6:00 (prophase) and ~13:00 (early prometaphase) before photoactivation. Layout is as in Figure 1. (B) A single optical plane of the early prometaphase cell in A reveals buckled microtubules (arrowheads). (C) Percentage of total motion plotted against rates. Setup is identical to Figure 1. Bar, 10 μm.

cannot result from microtubule treadmilling or centrosome separation, because marks on treadmilling microtubules would remain stationary (Rodionov and Borisy, 1997), and centrosome motion is insufficient to account for the observed motility (Supplemental Figure S2).

The argument for flux based on the kinesin-13 inhibition effect rests heavily on the assumption that microtubule minus ends localize to centrosomes, where they can engage with the Kif2a depolymerase. Although the location of minus ends in mammalian prophase arrays is unknown, the distribution of microtubules in deconvolved images of fixed cells shows that some minus ends seem to localize at centrosomes (Supplemental Figure S1B). Importantly, recent work in *Xenopus* egg extracts has suggested that microtubule minus ends in metaphase cells are not restricted to spindle poles; instead, they are distributed throughout the spindle length (Burbank *et al.*, 2006). One consequence of this cytoskeletal organization is that flux can proceed with only a subset of microtubule minus ends located at the spindle pole, a finding relevant to microtubule behavior in prophase arrays.

Although a definitive demonstration that microtubules in prophase cells undergo flux requires simultaneous imaging of a photoactivated mark on the microtubule lattice and visualization of the minus end of that microtubule, an experiment not presently possible due to the density of microtubules in mammalian prophase arrays, the response of slow P motion to inhibition of dynein and kinesin-13 proteins, and the above-mentioned arguments, strongly support the

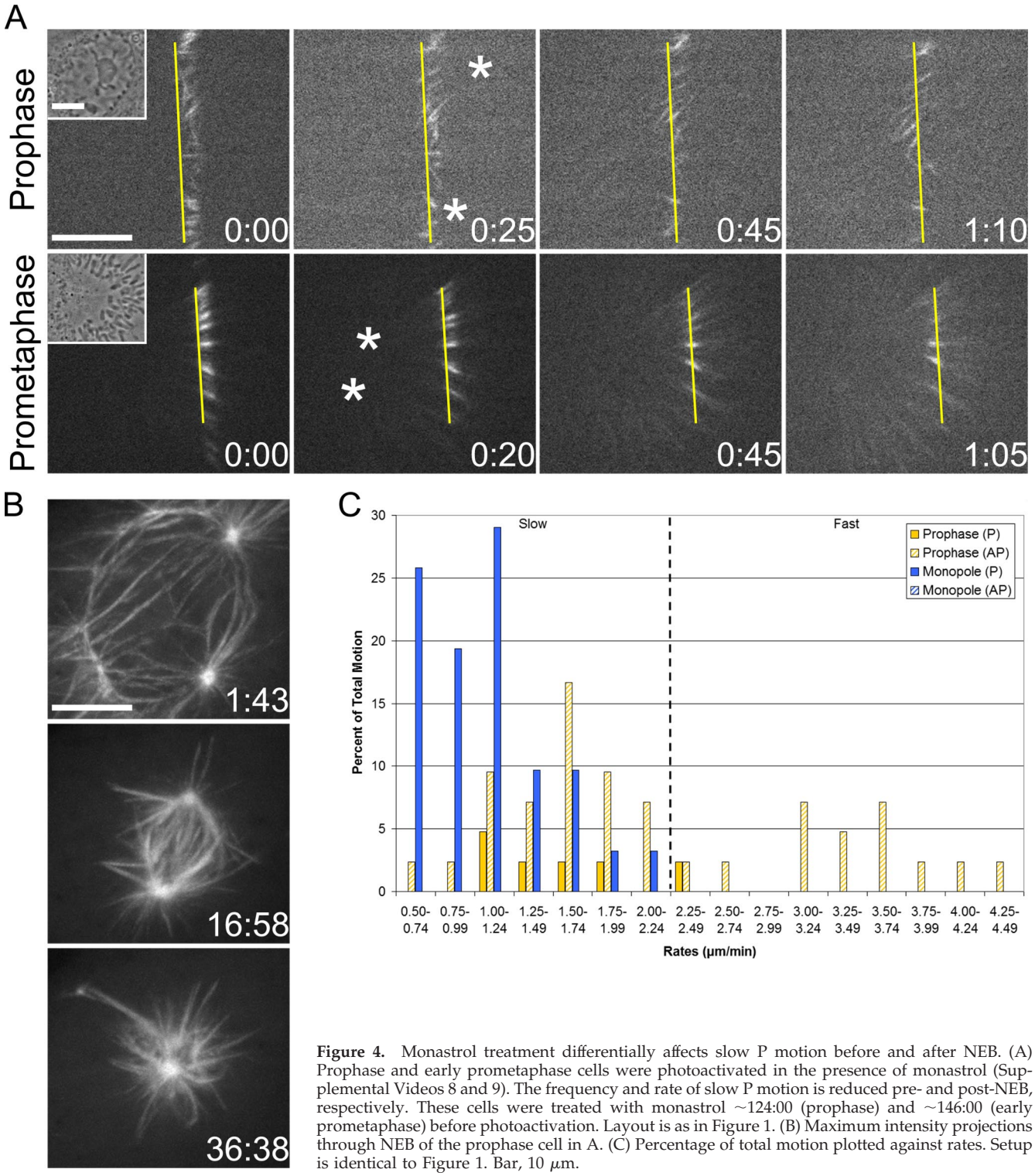

Figure 4. Monastrol treatment differentially affects slow P motion before and after NEB. (A) Prophase and early prometaphase cells were photoactivated in the presence of monastrol (Supplemental Videos 8 and 9). The frequency and rate of slow P motion is reduced pre- and post-NEB, respectively. These cells were treated with monastrol ~124:00 (prophase) and ~146:00 (early prometaphase) before photoactivation. Layout is as in Figure 1. (B) Maximum intensity projections through NEB of the prophase cell in A. (C) Percentage of total motion plotted against rates. Setup is identical to Figure 1. Bar, 10 μm.

hypothesis that early mitotic slow P motion represents flux. What then could be the role of such a phenomenon? We have previously shown that peripheral microtubules are moved inward toward the forming spindle in a dynein-dependent manner (Rusan *et al.*, 2002). Prophase flux could also contribute to inward motion, and it may serve as a backup or complementary mechanism to dynein-dependent sliding of peripheral microtubules.

What Accounts for the Variation of Prophase Microtubule Motion?

A major conclusion of our analysis of microtubule behavior is that there is a marked reduction in the variability of rates and directionalities from prophase (where slow and fast, P and AP motion is detectable), to early prometaphase (where slow and fast AP motion essentially disappears), to meta-

phase (where only slow P motion remains). We propose that the reduction in microtubule motion results not from changes in the active/inactive state of mitotic motors, but from progressive changes in microtubule organization during spindle formation. This possibility is supported by the fact that mitotic motors are activated as cells enter mitosis and Cdk1 activity rises, and they are thought to remain active until exit from mitosis (Verde *et al*., 1990, 1991; Blangy *et al*., 1997). Microtubule dynamics are similarly activated at entry into mitosis (Verde *et al*., 1990; Verde *et al*., 1992). Thus, the suppression of microtubule motion is likely to result from the progressive establishment of interactions between microtubules and spindle components (i.e., centrosomes and kinetochores) as well as from microtubule–microtubule interactions.

The clearest support for this possibility is the loss of fast microtubule motion as cells progress through mitosis. Our results demonstrate that fast motion is dynein dependent, yet substantial evidence supports the view that dynein remains active throughout mitosis. It is possible that only free, untethered microtubules (defined here as microtubules that are not linked, or weakly linked, to other microtubules, spindle poles, or kinetochores) undergo fast motion. In support of this, exogenous microtubule pieces added to asters in *Xenopus* extracts move rapidly poleward in a dynein-dependent manner, presumably because they are not tethered to spindle components (Heald *et al*., 1997). As mitosis progresses, free microtubules that are moved poleward by dynein could become tethered to the spindle pole by dynein/NuMA/dynactin complexes (Merdes *et al*., 1996). Conversely, microtubules that are moved away from the poles may undergo catastrophe and rapid disassembly in the peripheral cytoplasm (Rusan *et al*., 2001).

Progressive changes in microtubule organization may also account for the differential response of pre- and post-NEB cells to Eg5 inhibition. Our data support the possibility that Eg5 functions as both a feeder, delivering microtubules to the kinesin-13 depolymerase (Cassimeris, 2004; Gadde and Heald, 2004), and a tether, cross-linking neighboring microtubules (Kapitein *et al*., 2005). During prophase, other molecular components that would normally contribute to tethering may be unable to. NuMA, for example, plays a major role in organizing spindle poles (Merdes *et al*., 1996), but is nuclear, and therefore unavailable, in prophase cells (Compton *et al*., 1992). If Eg5 acts as the dominant tether during prophase, then monastrol treatment could result in microtubules becoming untethered, leading to the observed increase in the frequency of AP motion, because antagonistic motors can slide free microtubules. Importantly, although it is recognized that monastrol treatment does not disrupt Eg5–microtubule interactions (Kapoor *et al*., 2000), Eg5-bound microtubules are capable of sliding in the presence of monastrol (Crevel *et al*., 2004). After NEB, proteins other than Eg5 (i.e., NuMA) may tether spindle microtubules and Eg5 inhibition would not result in AP motion because these microtubules would remain tethered. Furthermore, Eg5 inhibition may limit the rate of flux-like motion in post-NEB, but not prophase cells, because its activity could be required to overcome antagonistic forces that oppose slow P motion (Sharp *et al*., 2000); such forces could come about, for example, through antiparallel microtubule cross-links, of which there are few in prophase.

Considering the increasing degree of coordination of microtubule motion from prophase to metaphase, it is an interesting possibility that the flux machinery is operational throughout all of mitosis and only becomes obviously apparent when other motion has been suppressed or eliminated, as the spindle matures.

ACKNOWLEDGMENTS

p150-CC1 plasmid was a kind gift of Dr. Tarun Kapoor. Antibodies were generously provided by Drs. Duane Compton (Kif2a and Eg5) and Claire Walczak (MCAK). We thank Dr. Wei-Lih Lee for helpful suggestions on this manuscript. This work was supported by a grant from the National Institutes of Health (to P.W.).

REFERENCES

Blangy, A., Arnaud, L., and Nigg, E. A. (1997). Phosphorylation by $p34^{cdc2}$ protein kinase regulates binding of the kinesin related motor HsEg5 to the dynactin subunit $p150^{glued}$. J. Biol. Chem. *272*, 19418–19424.

Burbank, K. S., Groen, A. C., Perlman, Z. E., Fisher, D. S., and Mitchison, T. J. (2006). A new method reveals microtubule minus ends throughout the meiotic spindle. J. Cell Biol. *175*, 369–375.

Cameron, L. A., Yang, G., Cimini, D., Canman, J. C., Kisurina-Evgenieva, O., Khodjakov, O., Danuser, G., and Salmon, E. D. (2006). Kinesin 5-independent poleward flux of kinetochore microtubules in PtK1 cells. J. Cell Biol. *173*, 173–179.

Cassimeris, L. (2004). Cell division: eg'ing on microtubule flux. Curr. Biol. *14*, R1000–R1002.

Compton, D. A., Szilak, I., and Cleveland, D. W. (1992). Primary structure of NuMA, an intranuclear protein that defines a novel pathway for segregation of proteins at mitosis. J. Cell Biol. *116*, 1395–1408.

Crevel, I. M., Alonso, M. C., and Cross, R. A. (2004). Monastrol stabilises an attached low-friction mode of Eg5. Curr. Biol. *1*, R411–R412.

DeLuca, J. G., Newton, C. N., Himes, R. H., Jordan, M. A., and Wilson, L. (2001). Purification and characterization of native conventional kinesin, HSET, and CENP-E from mitotic HeLa cells. J. Biol. Chem. *276*, 28014–28021.

Desai, A., Verma, S., Mitchison, T. J., and Walczak, C. E. (1999). Kin I kinesins are microtubule-destabilizing enzymes. Cell *96*, 69–78.

Gadde, S., and Heald, R. (2004). Mechanisms and molecules of the mitotic spindle. Curr. Biol. *14*, R797–R805.

Gaetz, J., and Kapoor, T. M. (2004). Dynein/dynactin regulate metaphase spindle length by targeting depolymerizing activities to spindle poles. J. Cell Biol. *166*, 465–471.

Ganem, N. J., and Compton, D. A. (2004). The KinI kinesin Kif2a is required for bipolar spindle assembly through a functional relationship with MCAK. J. Cell Biol. *166*, 473–478.

Ganem, N. J., Upton, K., and Compton, D. A. (2005). Efficient mitosis in human cells lacking poleward microtubule flux. Curr. Biol. *15*, 1827–1832.

Heald, R., Tournebize, R., Habermann, A., Karsenti, E., and Hyman, A. (1997). Spindle assembly in *Xenopus* egg extracts: respective roles of centrosomes and microtubule self-organization. J. Cell Biol. *138*, 615–628.

Kapitein, L. C., Peterman, E.J.G., Kwok, B. H., Kim, J. H., Kapoor, T. M., and Schmidt, C. F. (2005). The bipolar mitotic kinesin Eg5 moves on both microtubules that it crosslinks. Nature *435*, 114–118.

Kapoor, T. M., Mayer, T. U., Coughlin, M. L., and Mitchison, T. J. (2000). Probing spindle assembly mechanics with monastrol, a small molecule inhibitor of the mitotic kinesin, Eg5. J. Cell Biol. *150*, 975–988.

King, S. J., Brown, C. L., Maier, K. C., Quintyne, N. J., and Schroer, T. A. (2003). Analysis of the dynein-dynactin interaction in vitro and in vivo. Mol. Biol. Cell *14*, 5089–5097.

LaFountain, J. R., Jr., Cohan, C. S., Siegel, A. J., and LaFountain, D. J. (2004). Direct visualization of microtubule flux during metaphase and anaphase in crane-fly spermatocytes. Mol. Biol. Cell *15*, 5724–5732.

Maddox, P. S., Bloom, K. S., and Salmon, E. D. (2000). The polarity and dynamics of microtubule assembly in the budding yeast *Saccharomyces cerevisiae*. Nat. Cell Biol. *2*, 36–41.

Maddox, P., Desai, A., Oegema, K., Mitchison, T. J., and Salmon, E. D. (2002). Poleward microtubule flux is a major component of spindle dynamics and anaphase A in mitotic *Drosophila* embryos. Curr. Biol. *12*, 1670–1674.

Maiato, H., Khodjakov, A., and Rieder, C. L. (2005). *Drosophila* CLASP is required for the incorporation of microtubule subunits into fluxing kinetochore fibres. Nat. Cell Biol. *7*, 42–47.

Mayer, T. U., Kapoor, T. M., Haggarty, S. J., King, R. W., Schreiber, S. L., and Mitchison, T. J. (1999). Small molecule inhibitor of mitotic spindle bipolarity identified in a phenotype-based screen. Science *286*, 971–974.

Merdes, A., Ramyar, K., Vechio, J. D., and Cleveland, D. W. (1996). A complex of NuMA and cytoplasmic dynein is essential for mitotic spindle assembly. Cell *87*, 447–458.

Mitchison, T. J. (1989). Polewards microtubule flux in the mitotic spindle: evidence from photoactivation of fluorescence. J. Cell Biol. *109*, 637–652.

Mitchison, T. J., and Salmon, E. D. (1992). Poleward kinetochore fiber movement occurs during both metaphase and anaphase-A in newt lung cell mitosis. J. Cell Biol. *119*, 569–582.

Miyamoto, D. T., Perlman, Z. E., Burbank, K. S., Groen, A. C., and Mitchison, T. J. (2004). The kinesin Eg5 drives poleward microtubule flux in *Xenopus laevis* egg extract spindles. J. Cell Biol. *167*, 813–818.

Patterson, G. H., and Lippincott-Schwartz, J. (2002). A photoactivatable GFP for selective photolabeling of proteins and cells. Science *297*, 1873–1877.

Quintyne, N. J., Gill, S. R., Eckley, D. M., Crego, C. L., Compton, D. A., and Schroer, T. A. (1999). Dynactin is required for microtubule anchoring at centrosomes. J. Cell Biol. *147*, 321–334.

Rodionov, V. I., and Borisy, G. G. (1997). Microtubule treadmilling in vivo. Science *275*, 215–218.

Rogers, G. C., Rogers, S. L., and Sharp, D. J. (2005). Spindle microtubules in flux. J. Cell Sci. *118*, 1105–1116.

Rogers, G. C., Rogers, S. L., Schwimmer, T. A., Ems-McClung, S. C., Walczak, C. E., Vale, R. D., Scholey, J. M., and Sharp, D. J. (2004). Two mitotic kinesins cooperate to drive sister chromatid separation during anaphase. Nature *427*, 364–370.

Rusan, N. M., Fagerstom, C. J., Yvon, A. M., and Wadsworth, P. (2001). Cell cycle-dependent changes in microtubule dynamics in living cells expressing green fluorescent protein-alpha tubulin. Mol. Biol. Cell *12*, 971–980.

Rusan, N. M., Tulu, U. S., Fagerstrom, C., and Wadsworth, P. (2002). Reorganization of the microtubule array in prophase/prometaphase requires cytoplasmic dynein-dependent microtubule transport. J. Cell Biol. *158*, 997–1003.

Salina, D., Bodoor, K., Eckley, D. M., Schroer, T. A., Rattner, J. B., and Burke, B. (2002). Cytoplasmic dynein as a facilitator of nuclear envelope breakdown. Cell *108*, 97–107.

Sawin, K. E., and Mitchison, T. J. (1991). Poleward microtubule flux in mitotic spindles assembled in vitro. J. Cell Biol. *112*, 941–954.

Sharp, D. J., Brown, H. M., Kwon, M., Rogers, G. C., Holland, G., and Scholey, J. M. (2000). Functional coordination of three mitotic motors in *Drosophila* embryos. Mol. Biol. Cell *11*, 241–253.

Shirasu-Hiza, M., Perlman, Z. E., Wittmann, T., Karsenti, E., and Mitchison, T. J. (2004). Eg5 causes elongation of meiotic spindles when flux-associated microtubule depolymerization is blocked. Curr. Biol. *14*, 1941–1945.

Tulu, U. S., Rusan, N. M., and Wadsworth, P. (2003). Peripheral, non-centrosome-associated microtubules contribute to spindle formation in centrosome-containing cells. Curr. Biol. *13*, 1894–1899.

Verde, F., Berrez, J.-M., Antony, C., and Karsenti, E. (1991). Taxol-induced microtubule asters in mitotic extracts of *Xenopus* eggs: requirements for phosphorylated factors and cytoplasmic dynein. J. Cell Biol. *112*, 1177–1187.

Verde, F., Dogterom, M., Stelzer, E., Karsenti, E., and Leibler, S. (1992). Control of microtubule dynamics and length by cyclin A- and cyclin B-dependent kinases in *Xenopus* egg extracts. J. Cell Biol. *118*, 1097–1108.

Verde, F., Labbe, J.-C., Doree, M., and Karsenti, E. (1990). Regulation of microtubule dynamics by cdc2 protein kinase in cell-free extracts of *Xenopus* eggs. Nature *343*, 233–237.

Wadsworth, P., and Khodjakov, A. (2004). E pluribus unum: towards a universal mechanism for spindle assembly. Trends Cell Biol. *14*, 413–419.

Zhai, Y., Kronebusch, P. J., and Borisy, G. G. (1995). Kinetochore microtubule dynamics and the metaphase-anaphase transition. J. Cell Biol. *131*, 721–734.